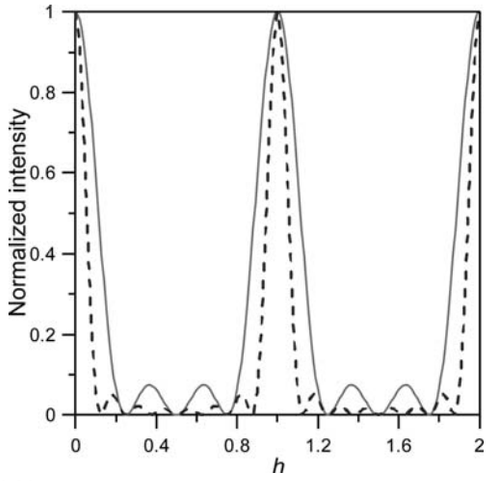

Figure 1.1.20
Normalized intensity from a finite lattice with $n = 3$ (solid curve) and $n = 8$ (dashed line), demonstrating the sharpening of peaks with increasing number of unit cells n. The normalization was done such that the peaks have the same peak maximum rather than the same integrated intensity for a clearer comparison of the relative peak widths.

vation of the Scherrer equation following Klug & Alexander (1974).

Fig. 1.1.21 shows the path-length difference *versus* the depth of the lattice plane. When the angle between the incoming beam and the lattice plane θ is different by an amount ε from the Bragg condition, it is always possible to find a lattice plane inside an infinite crystal where the extra path is $\Delta = \lambda(n + \frac{1}{2})$ for n integer, producing destructive interference. For a thick crystal this is true for arbitrarily small ε, which explains the sharp Bragg reflections. In the case of a crystal with finite dimensions, for small ε the plane for which $\Delta = \lambda(n + \frac{1}{2})$ holds will not be reached, thus leading to an intensity distribution over some small angular range. We can use this idea to estimate the broadening of a Bragg reflection due to size effects.

The thickness of a crystallite in the direction perpendicular to p planes of separation d_{hkl} (Fig. 1.1.21) is

$$L_{hkl} = pd_{hkl}. \tag{1.1.68}$$

The additional beam path between consecutive lattice planes at the angle $\theta + \varepsilon$ is

$$\begin{aligned}\Delta &= 2d\sin(\theta + \varepsilon)\\ &= 2d(\sin\theta\cos\varepsilon + \cos\theta\sin\varepsilon)\\ &= n\lambda\cos\varepsilon + 2d\sin\varepsilon\cos\theta\\ &\simeq n\lambda + 2d\sin\varepsilon\cos\theta.\end{aligned} \tag{1.1.69}$$

The corresponding phase difference is then

$$\delta\varphi = 2\pi\frac{\Delta}{\lambda} = 2\pi n + \frac{4\pi}{\lambda}\varepsilon d\cos\theta = \frac{4\pi\varepsilon d\cos\theta}{\lambda} \tag{1.1.70}$$

and the phase difference between the top and the bottom layer (layer p) is then

$$p\delta\varphi = p\frac{4\pi\varepsilon d\cos\theta}{\lambda} = \frac{4\pi L_{hkl}\varepsilon\cos\theta}{\lambda}. \tag{1.1.71}$$

Rearranging equation (1.1.71) leads to

$$\varepsilon = \frac{\lambda\delta\varphi}{4\pi L_{hkl}\cos\theta}, \tag{1.1.72}$$

which gives an expression for the misalignment angle in terms of the crystallite size L_{hkl} and the phase difference $\delta\varphi$ between the reflections originating from the top plane and the bottom plane. Clearly, the scattered intensity is at a maximum for $\delta\varphi = 0$ ($\varepsilon = 0$). With increasing ε the intensity decreases, giving rise to a peak of finite width. Perfect cancellation of the waves from the top and bottom planes occurs for a phase difference of $\delta\varphi = \pm\pi$, at which point $\varepsilon = \pm\lambda/(4L_{hkl}\cos\theta)$. On a 2θ scale, the measured angular width between these points is

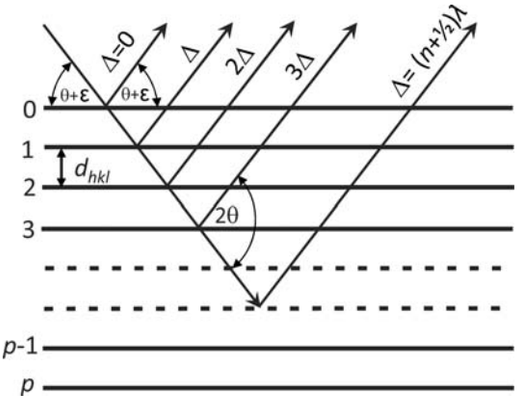

Figure 1.1.21
Path-length difference of the scattered ray *versus* the depth of the lattice plane in the crystal. [Reproduced from Dinnebier & Billinge (2008) with permission from the Royal Society of Chemistry.]

$$\beta_{hkl} = 4\varepsilon = \frac{\lambda}{L_{hkl}\cos\theta}, \tag{1.1.73}$$

giving us some measure of the peak width in radians that results from the finite particle size. A full treatment taking into account the correct form for the intensity distribution gives

$$\beta_{hkl} = \frac{K\lambda}{L_{hkl}\cos\theta}, \tag{1.1.74}$$

with a scale factor of $K = 0.89$ for perfect spheres. In general K depends on the shape of the grains (*e.g.* K is 0.94 for cube-shaped grains), but it is always close to unity. This equation is not valid for crystallites[3] that are too large or too small. In the case of large crystallites the peak width is governed by the coherence of the incident beam and not by particle size. For nanometre-sized crystallites, Bragg's law fails and the Debye equation needs to be used instead. The Debye equation (see Section 1.1.5.3) gives the scattering from an isotropically scattering sample such as a glass, liquid or powder, and does not presume that the sample is periodic.

1.1.4.1.2. *Microstrain*

Several important relationships in crystallography, including the effect of strain and microstrain on Bragg peaks, follow directly from a derivative of the Bragg equation (1.1.3). First we rewrite Bragg's law making the d-spacing the subject of the equation:

$$d = \frac{n\lambda}{2\sin\theta}. \tag{1.1.75}$$

The uncertainty of the measured lattice spacing is given by the total derivative dd,

$$\mathrm{d}d = \frac{\partial d}{\partial\theta}\mathrm{d}\theta + \frac{\partial d}{\partial\lambda}\mathrm{d}\lambda, \tag{1.1.76}$$

[3] Strictly speaking, the term crystallite size here refers to the dimension of a coherently scattering domain. Only in a perfect crystal is this the grain size.

Table 1.1.1
Types of scattering from a sample

Type of scattering	Coherent	Incoherent
Elastic	Bragg scattering Magnetic Bragg scattering Bragg scattering from ferroelectric/magnetic order Diffuse scattering from static defects Diffuse signal from small nanoparticles (<10 nm) Scattering from amorphous material (except excitations) Multiple scattering (coherent)	Laue monotonic diffuse scattering Neutron incoherent scattering Multiple scattering (incoherent)
Inelastic	Thermal diffuse scattering Spin-wave scattering Paraelectric/paramagnetic scattering Scattering from liquids	Compton scattering Fluorescence Incoherent scattering from hydrogen

leading to

$$\mathrm{d}d = -\frac{n\lambda}{2\sin\theta}\frac{\cos\theta}{\sin\theta}\mathrm{d}\theta + \frac{n}{2\sin\theta}\mathrm{d}\lambda \qquad (1.1.77)$$

and finally

$$\frac{\mathrm{d}d}{d} = -\frac{\mathrm{d}\theta}{\tan\theta} + \frac{\mathrm{d}\lambda}{\lambda}. \qquad (1.1.78)$$

When a crystal is strained, the d-spacings vary. A *macroscopic* strain changes the interplanar spacing by Δd_{hkl}, giving rise to a shift of $\Delta\theta$ in the *average* position of the diffraction peak. On the other hand, *microscopic* strains result in a distribution of d-spacings of width δd_{hkl}, which has the effect of *broadening* the diffraction peak by $\delta\theta$. Equation (1.1.78) gives an expression for the amount of Bragg-peak broadening that occurs for a given δd_{hkl}.

1.1.5. The background

1.1.5.1. *Information content in the background*

As discussed above, the elastic scattering from a crystalline powder consists of sharp rings, or peaks, of scattering at the 2θ angles where the Bragg or von Laue laws are satisfied. In general these sharp peaks sit on top of a 'background' which is broad and somewhat featureless. There are two components to this background, illustrated in Fig. 1.1.1: extraneous counts in the detector from things other than the sample, and non-Bragg scattering from the sample itself. The former are rarely of interest scientifically and the objective of a good experimental design is to minimize them as far as possible, or explicitly measure and subtract them, and then account well in any model or data interpretation for the part that cannot be eliminated from the measurement. Historically, the diffuse-scattering signals from the sample itself were also considered to be an inconvenience to be minimized and removed, and indeed in many cases this is still the best course of action (for example, sample fluorescence can be eliminated by choosing to work at an X-ray energy that lies below the absorption edge of a constituent atom). However, the diffuse 'background' from the sample can contain crucial information about defects, disorder and nanoscale order in the sample, and increasingly we are interested in studying it in order to understand the properties of the material that is under investigation. In some cases, such as glasses, liquids and samples of small nanoparticles, there is no Bragg scattering at all and only a diffuse scattering signal (see Chapter 5.6).

All the intensity scattered by the sample can be categorized as either coherent or incoherent and as elastic or inelastic, which are defined as follows. The coherency of the signal derives from whether or not the scattered waves interfere with each other constructively, and the resulting intensities are different in each case. For coherent scattering, the waves contributing to the signal are all summed first, before the wave amplitude is squared, to find the intensity distribution, which is the modulus squared of the resulting wave. For incoherent waves, one simply squares the amplitude of each wave to get its intensity and sums these together to get the total intensity. Switching to a consideration of the elasticity of the scattering, we define the scattering as elastic if the incident and scattered waves have the same energy, in which case no energy was exchanged during the scattering process between the incident wave and the sample, and inelastic scattering as the opposite. Inelastic scattering may result in a gain or a loss of energy of the scattered particle depending on the nature of the scattering, which results in a change in the wavelength of the scattered particle. There are also some non-scattering processes that can take place, such as absorption and fluorescence, but emissions resulting from these processes can also be categorized by whether or not they are coherent and elastic. It should be noted that the total energy of the system must be conserved during the scattering process, and so when a scattered wave gains or loses energy it exchanges it with the sample. This is used as a way of probing excitations in a material. Table 1.1.1 summarizes many of the types of diffuse scattering coming from a sample and categorizes them by their coherency and elasticity.

1.1.5.2. *Background from extraneous sources*

The most commonly observed extraneous, or parasitic, scattering is from the sample container (such as a capillary) that holds the sample during the measurement. Another large contribution may come from air scattering, which originates principally from scattering of the direct beam by molecules in the air in the beam path, both before and after the sample. Air-scattering effects can be minimized by enclosing as much of the beam path as possible in a tube which may be evacuated or where the air is replaced by a weakly scattering gas (such as He in the case of X-rays). Air scattering that is detected by the detector can also be reduced by careful collimation of the beams and then shielding the detector from detecting radiation that does not originate from the sample position. Collimating the incident beam is straightforward and results in a big reduction in air scattering. For point detectors it is also straightforward to collimate the scattered beam, but the modern trend towards using linear and area detectors makes this more difficult. There is sometimes a trade-off between collimating the scattered beam to reduce background and having uniform backgrounds that do not vary with angle because of